AUT Journal of Electrical Engineering

AUT J. Elec. Eng., 50(1)(2018)25-32
DOI: 10.22060/eej.2017.12312.5062

A Distributed Control Architecture for Autonomous Operation of a Hybrid AC/DC Microgrid System

R. Rahmani[1], A. Fakharian[2*]

[1]Qazvin Science and Research, Islamic Azad University, Qazvin, Iran
[2] Faculty of Electrical, Biomedical and Mechatronics Engineering, Qazvin Branch, Islamic Azad University, Qazvin, Iran

ABSTRACT: Hybrid AC/DC microgrids facilitate the procedure of DC power connection into the conventional AC power system by developing the distributed generations (DGs) technologies. The conversion processes between AC and DC electrical powers are more convenient by hybrid systems. In this paper, an energy management system (EMS) for a hybrid microgrid network is proposed due to the optimal utilization of renewable energy resources. EMS is designed based on two separate control parts, including proportional resonance (PR) and proportional integral (PI) controllers for managing the performance of two distribution generator (DG) and photo-voltaic (PV) sources. The novelty of implemented control scheme is the accurate prediction and recognition of load demand range with considering the DC bus voltage for coordinating the local sources. The advantage of this method is the proper control of both stable and transient states in power-sharing moments. The simulation results verify that the system outputs satisfy the load and power network requirements.

Review History:
Received: 31 December 2016
Revised: 9 August 2017
Accepted: 23 August 2017
Available Online: 1 October 2017

Keywords:
Hybrid microgrid management system (HMMS)
PI controller
PR controller
PV unit
stability

1- Introduction

Hybrid AC/DC microgrids will be the future energy distribution networks and a reliable alternative for existing AC power systems. An increase in the energy demand and black-out problems in conventional power networks are boosting the market and research attention towards distributed and renewable power generation systems like PV systems [1]. The technology advancements in renewable energy resources, power electronic interfaces and conversion methods provide broad utilization of DC power. It is required to guarantee the integration of this type of power with the conventional AC system. In the real world, hybrid microgrids facilitate the bi-directional conversion technology between AC and DC powers.

Distributed energy concept and decentralized control system cannot be implemented by the conventional power system. In general power network, there is an integrated network of generators, loads, and transmission lines. This topology establishes a power system with a high sensitivity to disturbances which occur in each part of the network. Hybrid microgrid enables the overall power network to be more flexible and reliable because of the islanded and connected operating modes and, also, convertible powers. The hybrid network can generate a large amount of DC power like PVs with the capability of conversion technologies. Hybrid microgrid provides acceptable reliability for the power systems and the required power quality for different loads. The considerable challenges in hybrid system with PV units are both basic and advanced issues related to harmonic control and stability and at the system level, synchronization with the grid, detection of islanding condition for PV power systems, and control under grid faults [2].

The corresponding author; Email: ahmad.fakharian@qiau.ac.ir

The major problem of a hybrid microgrid is the complexity of frequency and voltage control because of the absence of power grid in different working conditions and island modes especially. Another point is the method of pulse width modulation (PWM) switching to ensure the power quality by accurately converting both AC and DC powers. Therefore, the hybrid microgrid frequency and voltage control and also, the central controller (supervisory controller) schemes are almost the major challenges in the most of recent papers.

Some of these studies applied different methods and controllers for different designs of hybrid networks considered as possible future distribution structures [3],[4]. In [5], a voltage control strategy using a multi-PR controller is implemented to regulate the voltage of a multi-level inverter in the presence of uncertainties of the hybrid system. The paper [6] proposes a control method to remove the circulating current of the converter in the power sharing moments when a hybrid system is operated in an island mode. The proposed controller of this work includes a droop controller for autonomous power sharing and a virtual impedance controller for reducing the power sharing deviation. Also, a robust optimal power management system is developed for a hybrid AC/DC microgrid system in [7]. The DC bus voltage fluctuations are damped by a two-level controller which was used to consider the power of the battery banks. In the proposed strategy of [8], a multi-segment adaptive power/frequency characteristic curve adapts the power of a PV source in a hybrid unit. The control method is based on a multi-loop controller to provide a flexible operation of hybrid system in island mode.

The control of hybrid microgrid system depends on the structure of the network and the complexity of the controller, and various control methods were suggested in recent studies. Among the new schemes [9],[10], this paper works on a modern architecture of hybrid microgrid (renewable resources

as the main suppliers) and applies a novel hybrid microgrid management system (HMMS) based on the application of PR and PI controllers. In this study, a hybrid microgrid structure is designed for an automatic interconnection between different sources. A novel control plan is introduced to damp the system disturbances precisely and connect the sources of microgrid to each other with a high reliability and without any network failures in power sharing moments. In this way, the practicality and effectiveness of applied controller in the current study are examined and compromised with other studies. The prominent feature of the proposed scheme is the high response rate of HMMS to unpredicted changes. In the real world, the demand response concept has been realized correctly. This advantage is obtained by applying a hybrid controller composed of PI and PR controllers with different characteristics.

This paper studies the hybrid AC/DC microgrid system in island mode to control the system power sharing and load requirement. To survey the stability and reliability, the transient modes and disturbances are simulated by exchanging between six Z constant loads. The HMMS strongly associates with the system and PR and PI controllers' parameters. Therefore, the controllers' parameters are acquired by minimizing a proper cost function. The integrated time-weighted absolute error (ITAE) method is used to this end.

This paper is organized as follows. Section 2 involves the hybrid microgrid challenges in island mode. In this section, the routine power system circuit equations are represented for system analysis. In Section 3, the main structure of HMMS is discussed for load requirements in the island mode. Section 4 introduces a new control method based on the transient mode of PR and PI controllers. Section 5 shows the results of the implementation of this effective method for voltage control in this paper. In section 6, there is a synopsis argument on the control methods and uncertainties because of the various working modes.

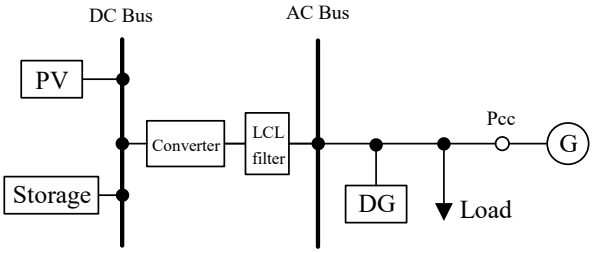

Fig. 1. Schematic diagram of hybrid AC/DC microgrid system

2- Problem Statement

We study a simulated model of a hybrid power network in the distributed level to represent a flexible system with a high reliability in all working modes. The control purpose is to damp the deviations of the AC and DC powers from nominal values. In some studies, e.g. [5], various types of controllers are applied to manage the operation of a hybrid system. To have an overview of the impact of each part of the controller on the system overall performance, the controller architecture has a modular structure. The control design for each converter is carried out individually and two similar PI controllers are proposed for the super capacitor (SC) and fuel cell (FC) controllers. Also, a multi-PR controller compensates for the harmonics of nonlinear loads to provide a regulated voltage. The main shortcoming of this scheme is the large close-looped transfer function of the system controller which increases the inertia of controller response. In addition, the PI and PR control parameters were not selected by the optimization algorithms.

In [3], inverter current control strategy was used to trigger the PWM inverter to supply the demanded AC or DC power. Although this model of controller has the ability to work in both island and connected modes, new control schemes are equipped with the island mode detection tools [13],[20]. Hence, the system frequency is fixed in the island mode and phase-locked loop (PLL) will be a useless block. In addition, PLL decreases the control system response rate because of the delay of its inner structure. Moreover, the proposed model includes two *abc-dq* transfer functions which generate extra harmonics and errors in control system responses.

Although the discussed studies proposed several models for hybrid microgrid systems, all requirements and criteria of power systems and loads are not satisfied or considered. In this study, the control idea is established based on a practical and efficient method to ensure the stability, reliability, and demand response. The analysis of the introduced controller performance is carried out in the island mode with a fixed frequency based on island detection ability. Therefore, a modern control concept is recommended using an accurate coordination between PI and PR controllers in a current control form in order to regulate the AC and DC bus voltages and also power sharing management in the hybrid mode.

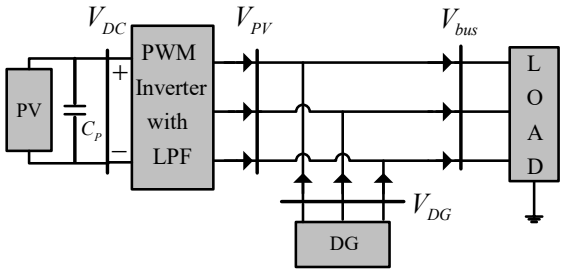

Fig. 2. 3-phase electrical diagram of hybrid system

Fig. 1 shows a sample hybrid AC/DC microgrid network. In this schematic diagram, the inner structure of the system is determined with a configuration of two AC and DC sources and loads. A PV source with energy storage system is connected to the DC bus and there is a DG source with AC load in AC bus. The total system is considered to operate in island mode.

Two mentioned buses are not separated from each other and the power sharing between them creates an integrated network. In the proposed schematic diagram, PV is the first source as a renewable energy supplier and DG has a supplementary role. The major problem for this island network is the regulation of AC and DC buses voltages and the correct power transformation between these buses considering the load demand.

Since the main function of the proposed hybrid microgrid is in AC system, all formulation and control design are made in AC framework. In order to analyze the operation of the proposed system, two scenarios are discussed for probable islanded operating modes. In these scenarios, PV is considered as the main source because of the utilization of renewable energy

resources; furthermore, DG is solely for critical conditions when the demanded power is higher than PV rated power.
In Fig. 2, an electrical diagram of PV and DG sources with AC load is shown. The mathematical formulation of 3-phase power circuit equations for this hybrid system is given by

- *Scenario 1: normal condition*

  When $I_{PV} = I_{bus}$ & $I_{DG} = 0$

$$P = \sqrt{3} V_{PV} I_{PV} \cos(\theta) \quad (1)$$

$$Q = \sqrt{3} V_{PV} I_{PV} \sin(\theta) \quad (2)$$

- *Scenario 2: critical condition*

  When $I_{bus} = I_{PV} + I_{DG}$

$$P = \sqrt{3} V_{bus} I_{bus} \cos(\theta) \quad (3)$$

$$Q = \sqrt{3} V_{bus} I_{bus} \sin(\theta) \quad (4)$$

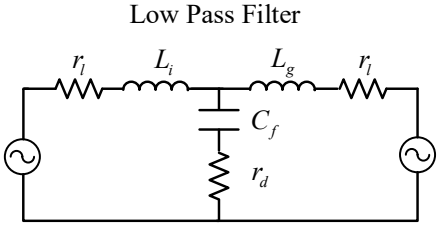

Fig. 3. Single line diagram of LPF

where P & Q are the exchanging active and reactive powers, respectively. θ is the power angle. V_{PV}, V_{DG} and V_{bus} are the root-mean-square (RMS) voltages of inverter output, DG source, and bus-bar. I_{PV}, I_{DG} and I_{bus} are the currents of PV, DG sources, and local load.

3- Hybrid Microgrid Management System (HMMS)

This paper improves the previous methods based on the system circuit equations which are combined with PI and PR controllers to respond the load demand. Here, a novel scheme of the current controller which has two series sections of PI and PR is introduced.

3- 1- PI Control Strategy

The first part of the control structure is a new application of a PI controller. In the hybrid systems, the DC bus voltage is a crucial index to recognize each change or disturbance in the network. The other advantage is that the DC bus voltage has definite values in normal and critical conditions and its variations in transient modes are a practical feedback for the control loop. Also, it is easier to control a DC parameter compared to AC one. Hence, the variations of DC bus voltage as V_{DC} are used for PI controller input. Considering that the general controller is modeled in 3-phase frame work, the DC value of PI controller output must be converted to AC analogue signal. Since the islanded hybrid network frequency is fixed on 50Hz, an AC reference signal can be generated for coupling the DC part to AC system. This signal as S_{ref} is applied to PI output. The PI control equation is defined as

$$I_{inv}^{ref} = S_{ref}(K_i \int (V_{DC}^{ref} - V_{DC})dt + K_p (V_{DC}^{ref} - V_{DC})) \quad (5)$$

where, K_i and K_p are the integral and proportional coefficients, respectively. The measured DC bus voltage is V_{DC} and V_{DC}^{ref} is the reference value which is set on 750V. I_{inv}^{ref} is the reference inverter current for the next PR controller.

3- 2- Determining the PR Controller Parameters

In order to start the design of the current controller, it is necessary to determine the type of appropriate controller. Proposed current controller applies a PR control strategy to precisely control the inverter parameters.
The PR controller includes two separate proportional and resonance parts which have a considerable influence on the overall performance of PR. The transfer function of this type of controller is described as:

$$PR = K_p^c + \frac{K_i^c s}{s^2 + 2\xi\omega_0 s + \omega_0^2} \quad (6)$$

In the transfer function of PR, ω_0 is the resonance frequency, thus, it value is equal to 50Hz. The value of K_i^c and ξ is strictly dependent on the behavior of transfer function in the condition that K_p^c is zero. Therefore, the variation of ξ is studied in the cases that K_i^c is assumed to be fixed and vice-versa. By assigning a range of numbers for both mentioned parameters, the result is that ξ must have a very low value (about zero), but the system frequency fluctuations are an obstacle for this hypothesis. Based on a trade-off between these two points, ξ is valued 0.01.
K_i^c has a direct impact on the system speed and inverse impact on the system error. It is assigned 10000 by try and error method.
The proportional factor K_p^c is associated with the system stability analysis. This means that the value of K_p^c must be selected while other parameters are given to assure the system stability. Therefore, K_p^c is calculated by surveying the stability of open loop transfer function (OLTF) in the next.

3- 3- Low Pass Filter

To remove the extra harmonics, a low pass filter (LPF) is embedded in the output of the inverter. The values of the LPF parameters are selected based on the filter designing methods [2]-[15]-[23]. In Fig. 3, a single line diagram of LPF is shown. Also, the values of the inverter and LPF parameters are determined in Table. 1.

Table 1. Parameters of inverter and LPF

Parameter	Value	Parameter	Value
$f_{switching}$	7 *kHz*	L_i	5*e*-3 *H*
f_{rated}	50 *Hz*	L_g	1*e*-3 *H*
V_{L-L}	380 v_{rms}	C_f	3*e*-5 *F*
P_{PV}	17 *KW*	r_d	5 Ω
P_{DG}	30 *KW*	C_P	5*e*-6 *F*

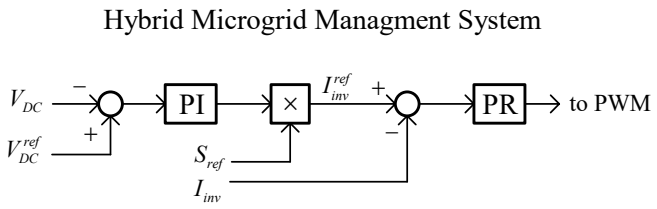

Fig. 4. Block diagram of HMMS for hybrid AC/DC system

4- NEW CONTROL METHOD

In [5], two current controllers were used based on the d-q technique. In each section, a PR controller was applied to control the *d*-axis and *q*-axis parameters. Two transformation processes were needed to *d-q*/*a-b-c* conversion, and, hence, the dimension of the control block diagram transfer function will be bigger and bring about an inapplicable system. This issue strongly decreases the system speed and increases the extra harmonics in the system signals through the *d-q*/*a-b-c* conversion. On the other hand, the new hybrid systems are equipped by island detection controllers to fix the system frequency on nominal value in island modes. Here, this has been done by generating a reference signal which is capable of setting all system AC signals, e.g. voltage and current, on nominal frequency.

As mentioned, the control scheme proposed in [5] is not capable to stabilize the system states in the accepted settling time which is defined in controlling processes while the end-user requires a fixed profile voltage and the nominal frequency with a high reliability in a very little time to pass the transient states. To establish such condition, this paper proposes a novel control scheme which includes HMMS with two different operations of PI and PR controllers.

The block diagram form of HMMS is shown in Fig. 4. In this design, I_{inv}^{ref} is the PI output which is a desirable current signal for PR.. To facilitate the control process and enhance the system response to the variations and disturbances, an applicable operation of PR control concept is proposed. The current control is designed for only one phase in a 3-phase reference framework. The controlling signals of the other phases are produced by a *3-phase module* which generates the 3-phase signals from one phase of PR output by shifting the angle input signal in 120 and 240 degrees.

Here, the OLTF is represented to survey the system stability. The formulation of this transfer function is given by

$$TF(s) = PI(s)PR(s)LPF(s) = (\mathrm{K}_P + \frac{K_i}{s})(K_p^c + \frac{K_i^c s}{s^2 + 2\xi\omega_0 s + \omega_0^2}) \quad (7)$$
$$(\frac{sC_f r_d + 1}{s^3 L_i L_g C_f + s^2 C_f r_d (L_i + L_g) + s(L_i + L_g)}).$$

As shown, the transfer function includes three sub transfer functions as PI, PR, and LPF and all parameters are specified except K_p^c. The procedure is that K_p^c is determined in a way to verify the system stability. According to the stability studies for OLTF, the K_p^c=100 satisfies the system stability from the control viewpoint. In addition, the selected control parameters support the system stability for both scenarios which were described in section 2.

In the following, the stability study is performed for two AC and DC working scenarios, which cover all probable modes of the hybrid system. The OLTF must be considered by parameters which are available in Tables I and II. The OLTF that is obtained from mathematical computation can be written as:

$$TF(s) = \frac{168.8\ s^4 + 1.421e06\ s^3 + 2.056e09\ s^2 + 5.388e11\ s + 2.776e13}{7.5e\text{-}07\ s^6 + 0.004505\ s^5 + 30.1\ s^4 + 632.6\ s^3 + 2.961e06\ s^2} \quad (8)$$

The poles of OLTF are obtained from (8) as:

$$X = [-68.9, -455.5, -1126.9 \pm 6798.3i, -1614 \pm 1537\,\mathrm{i}]$$

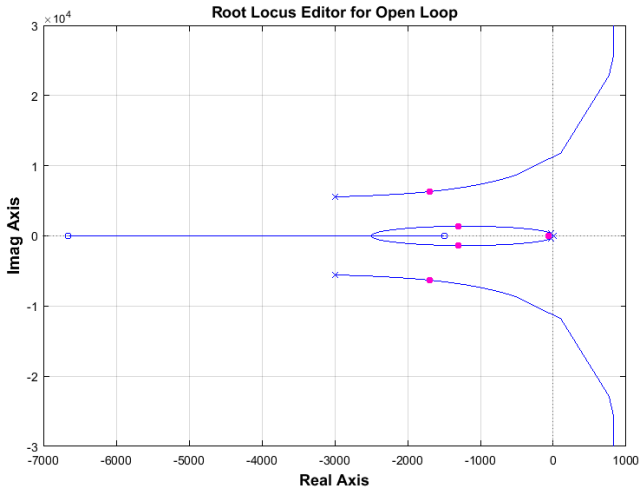

Fig. 5. Roots locus analysis for open loop transfer function when K_p^c=100

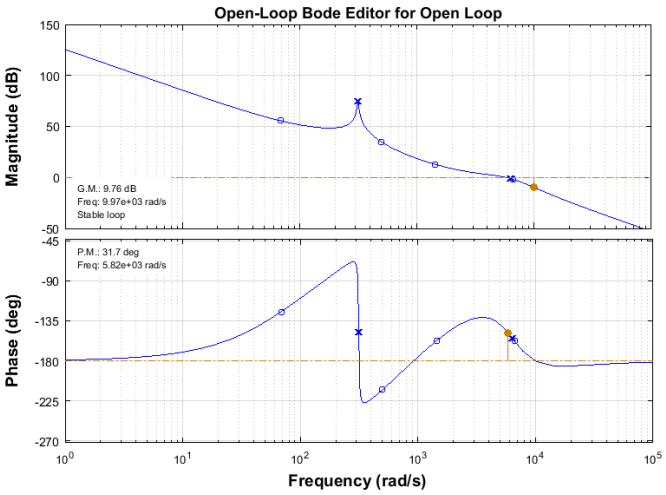

Fig. 6. Open-loop bode diagram for K_p^c=100

Fig. 5 shows the open-loop pole loci when all parameters are invariable and K_p^c is searched to have a value to confirm the system stability. According to the explanations above, the system sensitivity is controlled by K_p^c. Also, the bode diagram the OLTF when $K_p^c = 100$ is depicted in Fig. 6. As can be seen, the selected value for K_p^c preserves the system stability in a point in which the gain margin is 9.76 dB and the phase margin is 31.7 degree. These are acceptable values according to control texts.

A detailed structure of HMMS is displayed in Fig. 7. Generally, HMMS is formed by a combination of a DC bus controller and a current controller. The first part is a simple application

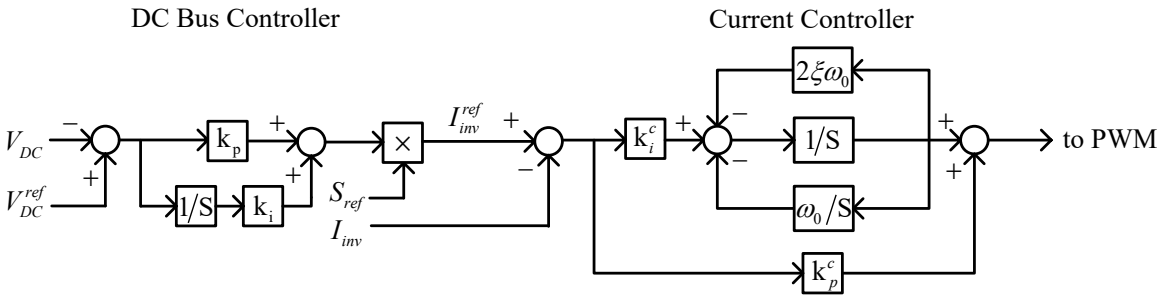

Fig. 7. Detailed control diagram of HMMS for a hybrid AC/DC microgrid network

of PI controller with two K_p and K_i control parameters. In the next part, the current controller works using a generated reference current by PI. The connector operator between DC and AC controller is S_{ref} Which is made by a sine wave with frequency 50 Hz. The PR controller parameters have a high impact on the performance of inverter in these types of hybrid system controllers. Therefore, it is essential to carefully check the system stability and its sensitivity to the variation of the PR controller parameters. These requirements will be evaluated in the next.

The significant characteristic of the proposed control scheme is to simplify the complexity of conventional hybrid system controllers by removing the extra $d-q/a-b-c$ transformations which were applied in previous papers. S_{ref} either links the DC and AC control parts or synchronizes the DG operation with PV unit. All the time, S_{ref} is applied to DG to prepare it for critical conditions and DG follows the angle of S_{ref} in all working modes.

5- Case Studies

This paper studies the control performance of HMMS in probable working mode. Actually, the case study is designed for surveying the power management strategy of DG and PV. To survey the performance of the proposed control structure, the system frequency is set on 50Hz for island mode, in addition, deviations of all AC and DC buses voltage are represented in all conditions which may exist in islanded hybrid systems. Two PI and PR controllers cover both AC and DC sub-grids. The reason for using DC parameters (like DC bus voltage) as inputs of PI controller is the fact that they have constant values and their variations are as step. Actually, V_{DC} is the best indicator for having a feedback of load behavior and system condition. In this methodology, the main challenge is transforming the AC and DC control parameters to each other without using a conventional *d-q* technique which is implemented in previous studies. Island detection technology in modern hybrid systems creates this capability to connect the AC and DC control environment just by generating a reference signal.

PR has the task of controlling the inverter current using a reference current which is supplied by PI controller. This part of current controller manages the AC parameters deviations by utilizing the PR characteristics.

Considering the proposed case study, the hybrid system works in these ways; the base source is PV due to the priority usage of renewable features and DG is a secondary resource. In the first scenario when demanded power is lower than the produced PV power, DG will be out of service and it injects no power to the system. In the next scenario, in which the consumable power exceeds the PV nominal power, DG is employed and synchronized with the system by the reference signal S_{ref}. The novelty of this study is the application of renewable energy resources as the main supplier while the DGs have this role in the similar networks of previous studies. The control parameters and power sharing values of sources and loads are represented in six simulated transient states in Table II. The coefficients of PI are set on values which are not the optimum values. The system output signals have a lower deviation by optimal values for PI control parameters. This discussion can be considered for future studies. To have a better view of the effectiveness of the proposed method, the crucial results of HMMS are represented.

Fig. 8 shows the active and reactive power variations of DG, PV and load considering the six load changes. The total simulation time is 1.8 seconds and for each variation, the values of active and reactive powers are strictly fixed on a given measure. The limited active power of PV is about 17KW. Therefore, the demanded power of more than this amount is provided by DG. In addition, when DG is in service, load reactive power is often supplied by DG. The exact values of DG, PV and load are represented in Table II.

In the first variation between 0-0.3, load active power is 20KW. PV injects its maximum power 17KW and the rest is provided by DG. As is clear in Fig. 8, DG approximately generates all load reactive powers. For the next variation between 0.3-0.6, the load active power goes below the PV rated power. Therefore, DG is out of service and the PV responds to the requested active and reactive power. This performance of the DG and the PV is exactly repeated for the various amounts of the load powers.

Fig. 9 shows the DC bus voltage amplitude varying between 750V and 850V. The profile of DC bus voltage is matched with the power-sharing procedure between sources. In this study, the PV unit operation is evaluated by the DC bus voltage. The normal DC voltage drop is limited by 750V when the load power raises above the PV nominal power. On the other hand, the requested load power reduction causes the controlled DC bus voltage to reaches at 850V. With this feedback of DC voltage, the PV unit can sense each working mode of the system and regulate its operation based on the available system condition and load requirement. Finally, the DC voltage 750V is for the maximum injected power by PV and 850V is for the reduced load demanded power under the PV rated power.

Table 2. Hybrid Microgrid Parameters

	Mode I	Mode II	Mode III	Mode IV	Mode V	Mode VI
time	0-0.3	0.3-0.6	0.6-0.9	0.9-1.2	1.2-1.5	1.5-1.8
K_p, K_i K_p^c, K_i^c ξ	0.02,5 100,450 0.01	0.02,5 100,450 0.01	0.02,5 100,450 0.01	0.02,5 100,450 0.01	0.02,5 100,450 0.01	0.02,5 100,450 0.01
P_{inv}, Q_{inv} P_{DG}, Q_{DG}	17,0.25 3,2.25	14,1 0,0	17,0.25 11,1.75	13,1.4 0,0	17,0.25 7,0.75	10,0 0,0
P_{load}, Q_{load}	20,2.5	14,1	28,2	13,1.4	24,1	10,0

(P_{rated}=30 KW,V_{rated}=380 V & f_{rated}=50 Hz)

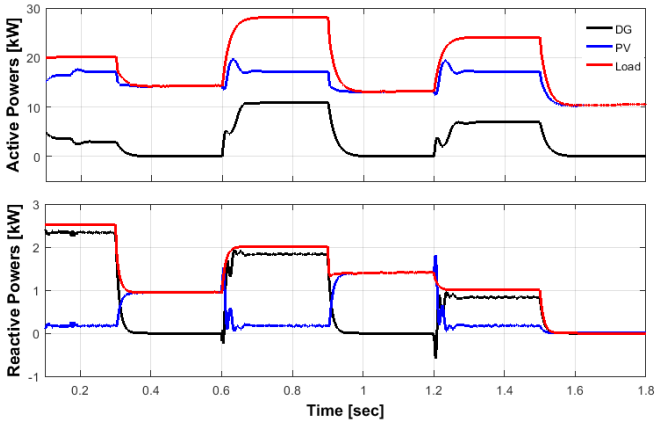

Fig. 8. Active and reactive powers of DG, PV, and load

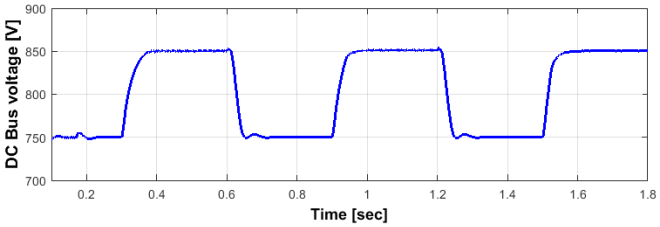

Fig. 9. DC bus voltage changes for HMMS operation

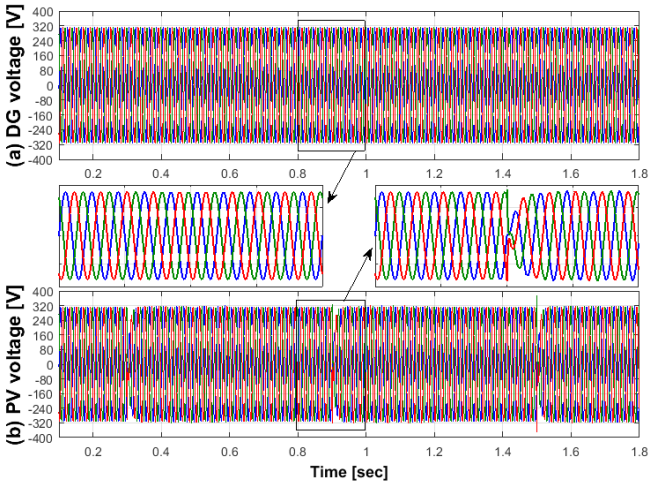

Fig. 10. Waveform of (a) DG and (b) inverter bus voltages

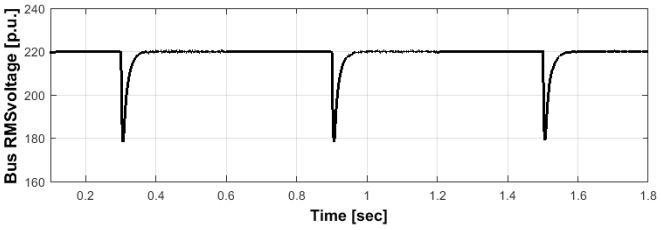

Fig. 11. AC bus RMS voltage transient deviations

In Fig. 10, the 3-phase DG and PV voltage is depicted for closely surveying the harmonics, frequency, and amplitude of power energy which is received by the end-user.

Fig. 11 shows the bus RMS voltage fluctuations based on the load changing. This scenario proves that the PI and PR controllers are able to firmly stabilize the voltage of hybrid microgrid system in each variation of working modes.

In Fig. 11, the bus voltage profile truly follows the changes in local load and becomes quickly stable on the nominal value. The bus voltage stays on 220V except in 0.3, 0.9 and 1.5 seconds. According to the 3-phase wavefroms which are represented for DG and PV voltage in Fig. 10, it is obvious that DG voltage is stable in all states and it is ready to just inject the required power to the system. Moreover, the PV voltage is set on the nominal voltage but it drops in the mentioned times in which PV solely supplies the load demand and DG is not in service. Hence, the fluctuation which exists in the bus voltage is due to the PV voltage. In fact, the bus voltage is an indication for hybrid microgrid system stability despite the many uncertainties in island mode.

The waveform of DG, PV and load currents are shown in Fig. 12 to clearly show the performance of the sources. Also, the supplementary role of DG is proved in the situations which consumed power by the load is provided by the PV unit when the DG current is zero.

Fig. 13 depicts the RMS currents of the hybrid system. Since the profile voltage for all AC buses is fixed on nominal value, the current behavior of DG, PV, and load is similar to the power waveform. This validates the studied hybrid microgrid system operation based on the power grid requirements.

Although the HMMS strongly depends on the system structure, the tested control scheme is applicable in expanded hybrid networks.

To investigate the operation of the HMMS, a comparison is made among the methods in [3], [5], and the proposed one in Table III. This analogy is based on both control and power system indexes. It is clear that HMMS totally has better simulation results for hybrid system.

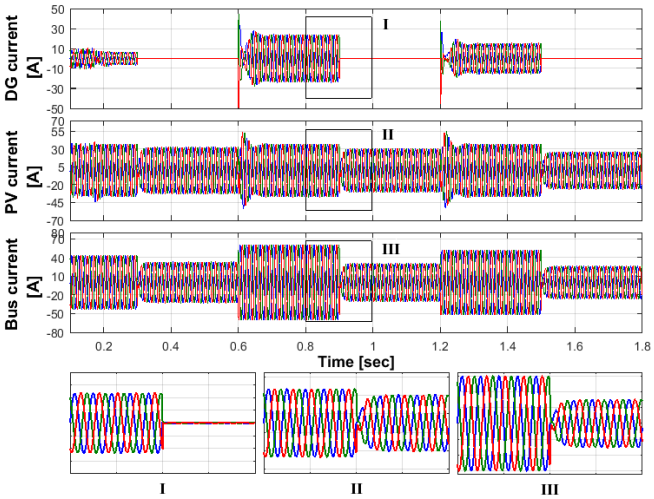

Fig. 12. 3-phase system performance based on exchanged currents

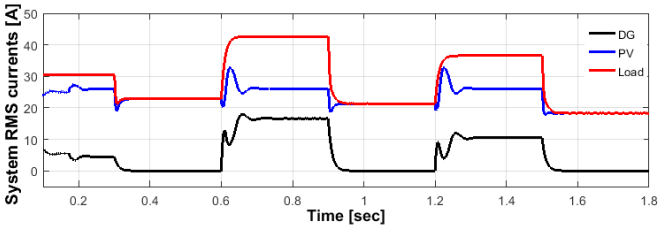

Fig. 13. RMS currents for hybrid system sources (DG&PV) and load

Table III. Comparison of results

	[3]	[5]	This study
Settling time	Medium (About 0.3 sec)	Low (About 2 sec)	Fast (Under 0.02 sec)
Over/Under shoots	Low (About 5%)	High (About 50%)	Low (About 10%)
Time for each change	1 sec	6 sec	0.3 sec
High-frequency harmonics	Low	High	Almost without harmonic
DC bus voltage fluctuations	Low	High	Low
Controller	Extra d-q transformation	Extra d-q transformation	3-phase framework
System response to changes	Medium	Slow	Fast

6- Conclusion

In this paper, a new control method was proposed based on the distributed approach for hybrid microgrid systems. The control scheme was a combination of two different PI and PR controllers for DC and AC frameworks. The proposed HMMS could compensate for the hybrid system disturbances and transient modes which were simulated by load changing. Also, verification of the system stability and reliability was precisely performed in different modes. The main focus of this study was on designing a practical architecture for hybrid microgrid systems to create a network for more participation of renewable energy resources in the modern power grids. The concentration of this study was on the control of island working mod and also island detection method for hybrid system. In this way, an integrated control scheme which consists of a DC and an AC controller was proposed. The practicality and the performance of the proposed method were verified by the simulation results.

References

[1] M. Liserre, R. Teodorescu, F. Blaabjerg, Stability of photovoltaic and wind turbine grid-connected inverters for a large set of grid impedance values, Power Electronics, IEEE Transactions on, 21(1) (2006) 263-272.

[2] R. Teodorescu, M. Liserre, P. Rodriguez, Grid converters for photovoltaic and wind power systems, John Wiley & Sons, 2011.

[3] P. Teimourzadeh Baboli, M. Shahparasti, M. Parsa Moghaddam, M.R. Haghifam, M. Mohamadian, Energy management and operation modelling of hybrid AC–DC microgrid, Generation, Transmission & Distribution, IET, 8(10) (2014) 1700-1711.

[4] F. Nejabatkhah, Y.W. Li, Overview of power management strategies of hybrid AC/DC microgrid, Power Electronics, IEEE Transactions on, 30(12) (2015) 7072-7089.

[5] M. Hamzeh, A. Ghazanfari, H. Mokhtari, H.R. Karimi, Integrating hybrid power source into an islanded MV microgrid using CHB multilevel inverter under unbalanced and nonlinear load conditions, Energy Conversion, IEEE Transactions on, 28(3) (2013) 643-651.

[6] H. Xiao, A. Luo, Z. Shuai, G. Jin, Y. Huang, An Improved Control Method for Multiple Bidirectional Power Converters in Hybrid AC/DC Microgrid, Smart Grid, IEEE Transactions on, 7(1) (2016) 340-347.

[7] M. Hosseinzadeh, F.R. Salmasi, Robust optimal power management system for a hybrid AC/DC micro-grid, IEEE Transactions on Sustainable Energy, 6(3) (2015) 675-687.

[8] H. Mahmood, D. Michaelson, J. Jiang, Decentralized Power Management of a PV/Battery Hybrid Unit in a Droop-Controlled Islanded Microgrid, Power Electronics, IEEE Transactions on, 30(12) (2015) 7215-7229.

[9] E. Unamuno, J.A. Barrena, Hybrid ac/dc microgrids—Part I: Review and classification of topologies, Renewable and Sustainable Energy Reviews, 52 (2015) 1251-1259.

[10] E. Planas, J. Andreu, J.I. Gárate, I.M. de Alegría, E. Ibarra, AC and DC technology in microgrids: A review, Renewable and Sustainable Energy Reviews, 43 (2015) 726-749.

[11] M. Hosseinzadeh, F.R. Salmasi, Power management of an isolated hybrid AC/DC micro-grid with fuzzy control of battery banks, Renewable Power Generation, IET, 9(5) (2015) 484-493.

[12] R. Rahmani, A. Fakharian, A combination of 3-phase

and dq techniques for controlling the islanded microgrid system: New schemes, in: Electrical Engineering (ICEE), 2015 23rd Iranian Conference on, IEEE, 2015, pp. 1457-1462.

[13] C. Li, C. Cao, Y. Cao, Y. Kuang, L. Zeng, B. Fang, A review of islanding detection methods for microgrid, Renewable and Sustainable Energy Reviews, 35 (2014) 211-220.

[14] P. Wang, C. Jin, D. Zhu, Y. Tang, P.C. Loh, F.H. Choo, Distributed control for autonomous operation of a three-port AC/DC/DS hybrid microgrid, Industrial Electronics, IEEE Transactions on, 62(2) (2015) 1279-1290.

[15] H. Bevrani, S. Shokoohi, An intelligent droop control for simultaneous voltage and frequency regulation in islanded microgrids, Smart Grid, IEEE Transactions on, 4(3) (2013) 1505-1513.

[16] C. Wang, X. Li, L. Guo, Y.W. Li, A nonlinear-disturbance-observer-based DC-bus voltage control for a hybrid AC/DC microgrid, Power Electronics, IEEE Transactions on, 29(11) (2014) 6162-6177.

[17] R. Majumder, A hybrid microgrid with DC connection at back to back converters, Smart Grid, IEEE Transactions on, 5(1) (2014) 251-259.

[18] N. Eghtedarpour, E. Farjah, Power control and management in a hybrid AC/DC microgrid, Smart Grid, IEEE Transactions on, 5(3) (2014) 1494-1505.

[19] M. Farhadi, O. Mohammed, Adaptive energy management in redundant hybrid DC microgrid for pulse load mitigation, Smart Grid, IEEE Transactions on, 6(1) (2015) 54-62.

[20] G. Bayrak, E. Kabalci, Implementation of a new remote islanding detection method for wind–solar hybrid power plants, Renewable and Sustainable Energy Reviews, 58 (2016) 1-15.

[21] R. Rahmani, A. Fakharian, New Control Method of Islanded Microgrid System: A GA & ICA based optimization approach, The Modares Journal of Electrical Engineering, 12(4) (2016) 43-52.

[22] S.J. Pinto, G. Panda, Performance evaluation of WPT based islanding detection for grid-connected PV systems, International Journal of Electrical Power & Energy Systems, 78 (2016) 537-546.

[23] S. Dhar, P. Dash, Adaptive backstepping sliding mode control of a grid interactive PV-VSC system with LCL filter, Sustainable Energy, Grids and Networks, 6 (2016) 109-124.

[24] S. Chowdhury, P. Crossley, Microgrids and active distribution networks, IET, 2009.

Please cite this article using:

R. Rahmani and A. Fakharian, A Distributed Control Architecture for Autonomous Operation of a Hybrid AC/DC Microgrid System, AUT J. Elec. Eng., 50(1)(2018) 25-32.

DOI: 10.22060/eej.2017.12312.5062